Bull. Chem. Soc. Jpn., 72, 2643—2653 (1999)

Characterization of CO- and H_2-Adsorbed Au_6Pt-Phosphine Clusters Supported on SiO_2 by EXAFS, TPD, and FTIR

Youzhu Yuan,† Kiyotaka Asakura,††,# Huilin Wan,† Khirui Tsai,† and Yasuhiro Iwasawa*

Department of Chemistry, Graduate School of Science, The University of Tokyo, Hongo, Bunkyo-ku, Tokyo 113-0033

†Department of Chemistry and State Key Laboratory for Physical Chemistry of Solid Surface, Xiamen University, Xiamen 361005, China

††Center of Spectrochemistry, Graduate School of Science, The University of Tokyo, Hongo, Bunkyo-ku, Tokyo 113-0033

(Received June 11, 1999)

The adsorption of CO and H_2 on a SiO_2-supported Au_6Pt cluster $[(AuPPh_3)_6Pt(PPh_3)](NO_3)_2$ (**1**) has been studied by means of FTIR, TPD, and EXAFS. CO adsorbed on **1**/SiO_2 to form a CO-adduct complex, which exhibited an IR band at ca. 1972 cm^{-1}. The adsorbed CO was desorbed below 403 K, showing a peak maximum at 363 K in TPD. There was little change in the coordination number of Pt–Au in Pt L_3-edge EXAFS upon CO adsorption, but the coordination number of Au–Au in Au L_3-edge EXAFS slightly increased and the peak ascribed to Pt–(Au)–P in the Pt L_3-edge EXAFS Fourier transform remarkably increased. The increase in the intensity of the Pt–(Au)–P peak was interpreted by the multiple scattering effect owing to the change of Pt–Au–P bond angle. The original EXAFS oscillations at both Pt and Au L_3-edges were regenerated after evacuation of the CO-adsorbed sample for 2 h at 353 K, indicating the recovery of the original cluster structure. This is entirely different from the case of the cluster **1** in solution, where the cluster framework is fragmented by the CO adsorption-desorption process. The adsorption of H_2 on **1**/SiO_2 was totally reversible at room temperature; it provided no contribution to the EXAFS oscillation.

Supported gold and gold–noble metal catalysts have attracted considerable attention from chemical interests as well as from the viewpoint of industrial applications.[1—3] It has been reported that the addition of gold to Pt catalysts increases catalytic activity and selectivity and suppresses deactivation in hydrocarbon conversions.[4—11] Recently, a SiO_2-supported cluster $[(AuPPh_3)_6Pt(PPh_3)](NO_3)_2$ (**1**) with a unique structure of a Pt atom embedded in a six Au-atoms ensemble was found to show significant catalysis for H_2–D_2 equilibration at 303 K, whereas a supported mononuclear Pt complex $Pt(PPh_3)_4/SiO_2$ and a supported Au cluster $[Au_6]^{2+}/SiO_2$ showed almost no activity for the H_2–D_2 exchange reaction.[12—15] This observation may be of interest because multi-sites composed of several Pt atoms are believed to be active sites for dihydrogen activation and H_2–D_2 equilibration on Pt particle catalysts.

It has also been reported that H_2 coordination on both **1** and $[(AuPPh_3)_8Pt(PPh_3)](NO_3)_2$ (**2**) rapidly and reversibly occurs:[16,17] $\{(Au)_nPt\}+H_2 \rightleftharpoons \{(Au)_nPt(H_2)\}$. Although $\{(Au)_nPt(H_2)\}$ is likely to be an intermediate in the catalytic H_2–D_2 equilibration, no structural information for this complex has been reported. Detailed NMR studies have been carried out with $\{(Au)_nPt\}$ (n = 6,7,8) clusters in solution.[17] In the case of **2**, the triple Pt–H coupling pattern was observed in the ^{31}P decoupled ^{195}Pt NMR spectrum, indicating the presence of two hydride ligands.[17] Since no terminal Pt–H stretching vibrations were detected by IR, the hydride ligands were assigned as bridge-bonding type.[18] In the case of **1** in CD_2Cl_2 solution, however, no changes in the NMR spectra have been observed.[17] In a basic solution like pyridine, deprotonation from $\{(Au)_n–Pt(H_2)\}$ to monohydrido cluster $\{(Au)_n–Pt(H)\}$ was directly observed by $^{31}P\{^1H\}$ NMR and ^1H NMR, which demonstrates that H_2 is activated to dissociate to H atoms on **1**.[16,19,20]

The catalytic H_2–D_2 equilibration on **1**/SiO_2 is completely suppressed by CO adsorption on the Pt atom of **1**/SiO_2. The adsorbed CO creates a site blocking effect as well as an electronic effect on the catalysis of **1**/SiO_2. However, there is no information on any structural change of the supported cluster framework upon CO adsorption.

The adsorption and reactivity of metal organic and inorganic compounds on oxide surfaces have been extensively studied to gain a better understanding of the fundamental principles of surface catalysis and the relations among bonding, structure and reaction.[21—24] This class of catalysts prepared by well-defined precursors has a great advantage in accepting the characterization of catalytically active structures and compositions by physical techniques. Among the characterization techniques, extended X-ray absorption fine structure (EXAFS) spectroscopy is of great importance for the structural study of dispersed metal sites on oxide surfaces in the static state and during the course of catalysis.[25,26] In-situ EXAFS analysis provided information on the bonding

Present address: Catalysis Research Center, Hokkaido University, Kita-ku, Sapporo 060-0811, Japan.

feature of Pt–Au(Pt) and Pt(Au)–ligands (such as phosphine and CO) in **1**/SiO_2.[13,15,27] We found a reversible change of the cluster structure induced by CO adsorption, which is different from the cluster fragmentation in solution.[27] In this paper, we report the further investigation on the structural change of **1**/SiO_2 upon adsorption and desorption of CO and H_2 by means of in-situ EXAFS, TPD (temperature programmed desorption), and FTIR.

Experimental

Preparation of the SiO_2-supported $[(AuPPh_3)_6Pt(PPh_3)](NO_3)_2$ (**1**) catalyst has been reported elsewhere.[13,15] The loading of **1** on SiO_2 was controlled to be 0.5—1.0 wt% based on Pt. All the procedures for sample preparation were conducted in Ar atmosphere (purity: 99.999%) to avoid contacting air. Adsorptions of CO and H_2 were measured in a closed circulating system at 298 K. The uptake was monitored at an interval of every 15 min until the pressure did not change, typically for about 40 min. The uptake of H_2 on **1**/SiO_2 was somewhat difficult to measure due to the weak interaction between H_2 and **1**/SiO_2 at 298 K. The data for H_2 adsorption have larger errors than those for CO adsorption. The H_2 adsorption was reversible.

Temperature-programmed desorption (TPD) spectra were measured in a fixed-bed reactor system equipped with a gas chromatograph. A dry-ice/acetone trap was used to eliminate the influence of water and hydrocarbons. The samples were first treated at room temperature for 120 min under Ar and then switched to CO (99.999%) for 10 min in a flow of 30 ml min^{-1}. After the sample was purged by Ar at a flow rate of 30 ml min^{-1} for 60 min, CO-TPD spectra were obtained with the carrier gas of Ar at a heating rate of 10 K min^{-1}.

IR spectra were measured on a JEOL JIR 7000 spectrometer with a resolution of 4 cm^{-1}. A pressed SiO_2 disk was placed in an IR cell with two NaCl windows, combined with a closed circulating system. The disk was pretreated at 673 K for 1 h in the cell and a dried ethanol solution of **1** was carefully added dropwise onto the disk in a flow of high-purity Ar. The supported sample was evacuated at 298 K for 4 h in-situ before CO adsorption. The spectra were recorded as difference spectra between before and after CO adsorption.

EXAFS measurements were carried out at BL-10B (for CO adsorption) and at BL-7C (for H_2 adsorption) of the Photon Factory in the Institute for Material Structure Science (PF-IMSS) (Proposal No. 95G200) operated at 2.5 GeV with a ring current 250—350 mA. The incident and transmitted X-rays were monitored by ionization chambers filled with N_2 and Ar (15%)–N_2 (85%) gases, respectively. EXAFS data were measured at room temperature in a transmission mode. The samples was transferred to an in-situ EXAFS glass cell by a Schlenk technique and evacuated at room temperature for 4 h. After recording the EXAFS spectrum of the sample, CO of 300 Torr (1 Torr = 133.322 Pa) was admitted into the EXAFS cell to measure the EXAFS spectrum for CO-adsorption sample. Then, the cell was evacuated at 353 K for 0.5 h and EXAFS was measured again. Similarly, the EXAFS measurement of H_2 adsorbed sample was carried out, but the measurement was conducted under 0.3 MPa of H_2.

The analysis of EXAFS was performed by removal of background using cubic smoothing and normalization with the edge height, whose energy dependency was taken into account using the McMaster equation.[28] The inverse Fourier-transformed EXAFS data were analyzed by a curve fitting method using phase-shifts and amplitudes calculated by the FEFF 6.01 software.[29] The parameters used for the FEFF calculations are listed in Table 1. The cluster **1**, Pt foil, Au foil, $Pt(PH_3)_4$ and $Au(PH_3)_4$ were used to determine the amplitude reduction factor S and to check the validity of these theoretically derived parameters. In the present analysis we took into account the error estimations recommended by the international XAFS workshop on standards and criteria.

Results

FT IR Spectra. When CO was admitted into **1**/SiO_2 in an in-situ IR cell, a single CO band at ca. 1972 cm^{-1} was observed, as shown in Fig. 1A. This is assigned to linear CO adsorbed on Pt. This is similar to the IR band at ca. 1967 cm^{-1} for $[(AuPPh_3)_6Pt(CO)(PPh_3)]^{2+}$ in solution.[30] Evacuation of the system caused a gradual decrease in the peak intensity, but the peak was still observable after evacuation for 4 h (Fig. 1A). The adsorbed CO can be completely removed by evacuation at 353 K (Fig. 1A-g).

When the **1**/SiO_2 sample was treated at 473 K in vacuum, the peak of adsorbed CO was observed at 1975 cm^{-1} (Fig. 1B). The previous EXAFS study indicated a small change in the cluster framework by the treatment at 473 K.[15] The IR peak frequency is slightly higher than that for the untreated sample; this may be related to a small structural change of the cluster **1** on SiO_2.

Adsorption of CO and H_2. Figure 2A shows irre-

Table 1. Crystallographic Data for the FEFF Calculation and Fourier Transform Ranges Used in the EXAFS Analysis

	FEFF Calculation		Fourier transformation range	
Bond	N	r/nm	Δk/nm^{-1}	Δr/nm
Pt–P for $Pt(PPh_3)$	1.0	0.228	30—90	0.14—0.23
Pt–Au for Pt(Au)	1.0	0.267	30—90	0.24—0.32
Pt–Pt for Pt foil	1.0	0.278	30—90	0.24—0.32
Pt–C for Pt(CO)	1.0	0.198	30—90	0.14—0.20
Pt–(C)–O for Pt(CO)	1.0	0.304	30—90	0.14—0.32
Pt–(Au)–P for Pt(Au–P)	1.0	0.497	30—90	0.39—0.50
Au–P for $Au(PPh_3)$	1.0	0.230	30—130	0.14—0.23
Au–Au for Au(Au) or Au(Pt)	1.0	0.287	30—130	0.24—0.32
Au–Au for Au foil	1.0	0.287	30—160	0.21—0.32

N: coordination number for absorber-backscatterer pair; r: interatomic distance; Δk: wavenumber range for forward Fourier transformation; Δr: distance range for shell isolation.

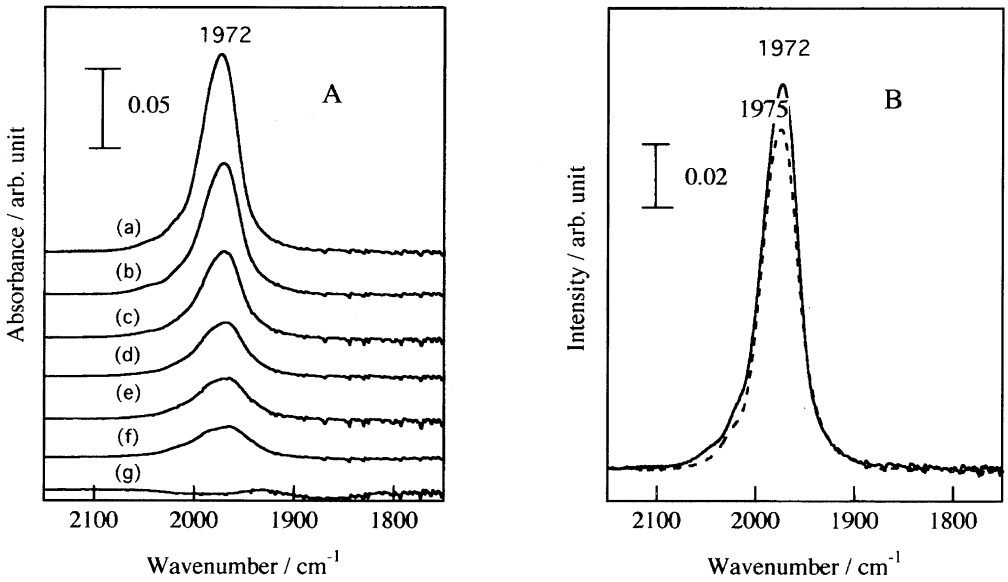

Fig. 1. FT-IR spectra for CO adsorbed on the intact **1**/SiO_2 (A) and the 473 K-treated **1**/SiO_2 (B); Evac. at RT for (a) 0 min; (b) 5 min; (c) 10 min; (d) 30 min; (e) 60 min; (f) 120 min; (g) Evac. at 353 K.

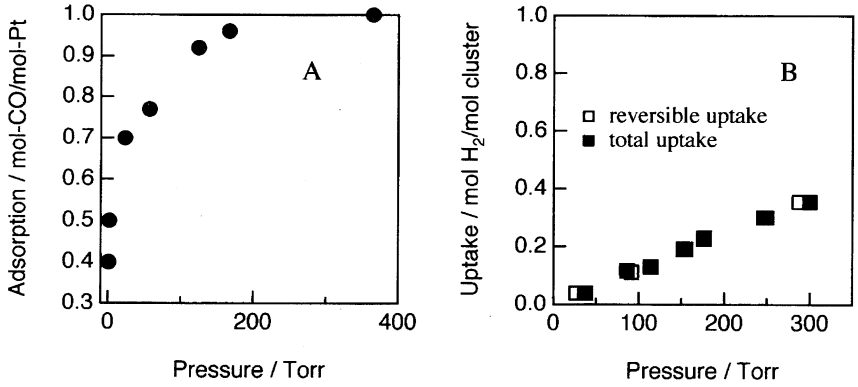

Fig. 2. The adsorption of CO (A) and H_2 (B) on **1**/SiO_2 at 298 K.

versible CO adsorption on **1**/SiO_2 at 298 K as a function of CO pressure. The CO uptake seems to be explained by the Langmuir adsorption isotherm. The amount of the irreversible adsorption was calculated by subtracting the amount of CO adsorbed in the second run from that in the first run. The system was evacuated at 298 K for 20 min between the first and second runs. The CO adsorption saturated at CO pressure of ca. 250 Torr, in which the coverage was one CO per Pt.

The result of H_2 adsorption on **1**/SiO_2 at 298 K is shown in Fig. 2B. The amount of adsorbed H_2 was very low. The adsorption isotherms show that hydrogen adsorption is completely reversible at 298 K.

CO-TPD on 1/SiO_2. CO-TPD spectra for **1**/SiO_2 untreated and treated at 473, 573, and 773 K are shown in Fig. 3. The TPD spectra for the intact **1**/SiO_2 and the 473 K-treated **1**/SiO_2 were similar to each other, whereas that for the 773 K-treated sample showed almost no peak in the same temperature range. In fact the CO uptake on the 773 K-treated sample was negligible. From the TPD data, we find that the CO uptakes on the intact and 473 K-treated samples were CO/Pt = 1.0 and 0.8, respectively.

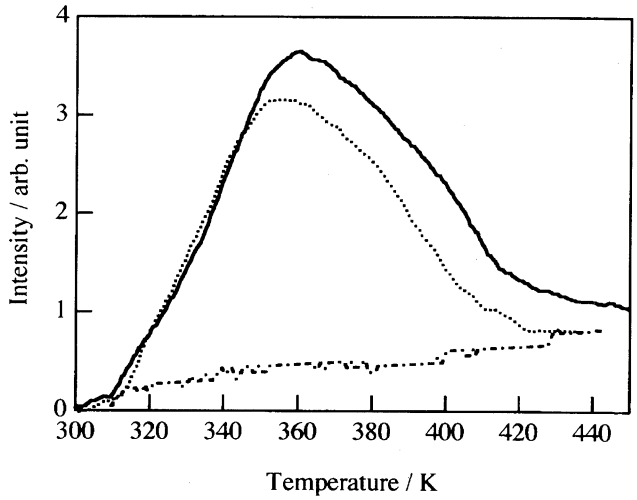

Fig. 3. CO-TPD of **1**/SiO_2.
— **1**/SiO_2; ···· **1**/SiO_2 pretreated at 473 K; –·– **1**/SiO_2 pretreated at 773 K.

EXAFS Measurements for CO-Adsorbed 1/SiO_2. We measured the Pt L_3-edge EXAFS spectra of **1**/SiO_2 before exposure to CO, after exposure to 300 Torr of CO and after evacuation at 353 K. The EXAFS oscillations and associated Fourier transforms are shown in Fig. 4. The peaks in the Fourier transforms that appeared in the range 0.1—0.35 nm are due to Pt–P and Pt–Au bondings. A small peak around 0.45 nm may be due to Pt–(Au)–P interaction. When **1**/SiO_2 was exposed to 300 Torr of CO at room temperature, the intensity of the peak at 0.45 nm became more than twice that for **1**/SiO_2, indicating that some change occurred with the Pt–(Au)–P bonding. When the CO-exposed **1**/SiO_2 was subsequently evacuated at 353 K, no decomposition of the framework of the Au_6Pt cluster was observed, but the peak at 0.45 nm reduced significantly, as shown in Fig. 4C.

Since the Pt–P and Pt–Au peaks are well separated from each other, they can be analyzed by a curve fitting method. The curve fitting analysis by two shells (Pt–P and Pt–Au) in the Fourier transform range 0.14—0.35 nm reproduced the experimental results for the intact **1**/SiO_2 and the evacuated **1**/SiO_2, as shown in Figs. 5A and 5C. The best-fit results are listed in Table 2. However, the two-shell fitting analysis for the CO-adsorbed sample never reproduced the experimental data. Therefore, we performed 4-term curve fitting analysis (Pt–C, Pt–P, Pt–Au, and Pt–(C)–O) adding a CO molecule coordinated to Pt. This analysis requires 16 fitting parame-

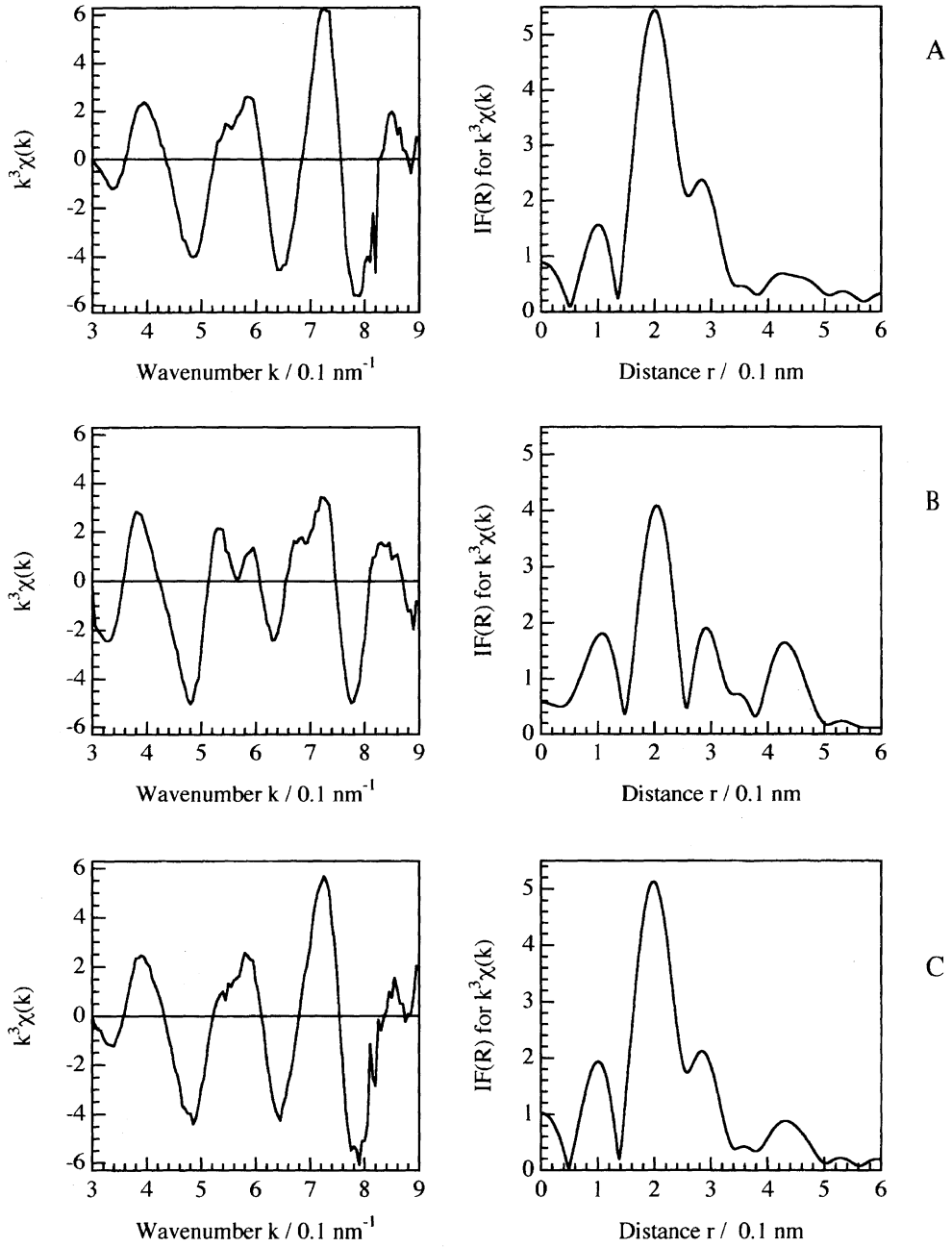

Fig. 4. Pt L_3-edge EXAFS oscillations and associated Fourier transforms for **1**/SiO_2. (A) **1**/SiO_2; (B) **1**/SiO_2 under 300 Torr of CO; (C) **1**/SiO_2 after evacuation at 353 K.

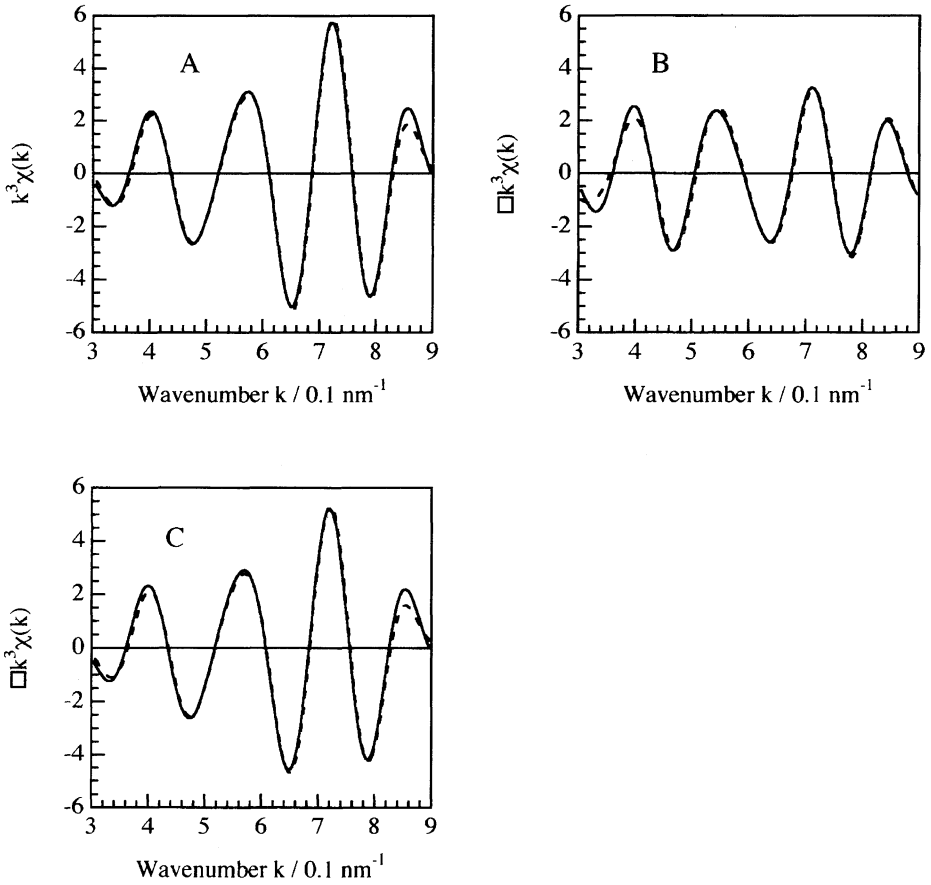

Fig. 5. The curve-fitting analysis for the Pt L_3-edge EXAFS data of **1**/SiO_2 based on two-shells (Pt–P and Pt–Au) model (A and C) and four-shells (Pt–C, Pt–P, Pt–Au, and Pt–(C)–O) model (B): —, observed, ····, calculated.
(A) **1**/SiO_2; (B) after CO adsorption; (C) after desorption of the adsorbed CO at 353 K.

Table 2. Curve-Fitting Results for the Pt L_3-edge EXAFS Data of **1**/SiO_2

Sample	Pt–P		Pt–Au	
	N	r/nm	N	r/nm
1	1[a)]	0.228[a)]	6[a)]	0.268[a)]
3	1[a)]	0.234[a)]	6[a)]	0.269[a)]
1/SiO_2	1.1±0.1	0.228±0.001	6.0±0.5	0.268±0.001
1/SiO_2 after adsorption of CO	1.2±0.4	0.231±0.004	5.8±0.9	0.269±0.003
1/SiO_2 after desorption of CO	1.1±0.1	0.229±0.001	5.9±0.5	0.269±0.001

The Δr range for the inverse Fourier transformation was 0.12—0.35 nm for both Pt and Au EXAFS. The curve fitting range was 30—90 nm^{-1} for Pt EXAFS. a) The averaged values derived from crystallographic data.[30] b) The bond distances for Pt–C and Pt–(C)–O were 0.194 and 0.309 nm, respectively.

ters more than the maximum number of degrees of freedom ($2\Delta r\Delta k/\pi \approx 10$). To conduct the analysis we fixed ΔE and σ values. The best-fit result is shown in Fig. 5B. The curve-fitting analysis data in Table 2 demonstrate the retention of the Pt–P and Pt–Au bondings in all the samples.

Figure 6 shows the EXAFS data at Au L_3-edge. The curve-fitting result is shown in Fig. 7A. Fig. 6B shows the EXAFS oscillation and its Fourier transform for **1**/SiO_2 exposed to 300 Torr of CO. No change in the intensity of the first peak attributable to Au–P was observed. The curve-fitting analysis revealed that Au–P and Au–Pt coordination numbers remained unchanged at nearly unity (Table 3). The Au_6Pt cluster framework was maintained with a small deformation after CO adsorption. Figure 6C shows the EXAFS oscillation and its associated Fourier transform for **1**/SiO_2 after CO desorption by evacuation at 353 K. The coordination number of Au–Au decreased to the same value as that for the intact **1**/SiO_2 (Table 3). It is concluded that the original structure of **1**/SiO_2 was recovered after desorption of CO.

EXAFS Measurements for H_2-Adsorbed 1/SiO_2. Since the adsorption of H_2 on **1**/SiO_2 was weak and small at room temperature, the EXAFS spectra for **1**/SiO_2 exposed to H_2 were measured under 0.3 MPa of H_2. Figures 8 and 9 (A, B, and C) show the oscillations and associated Fourier

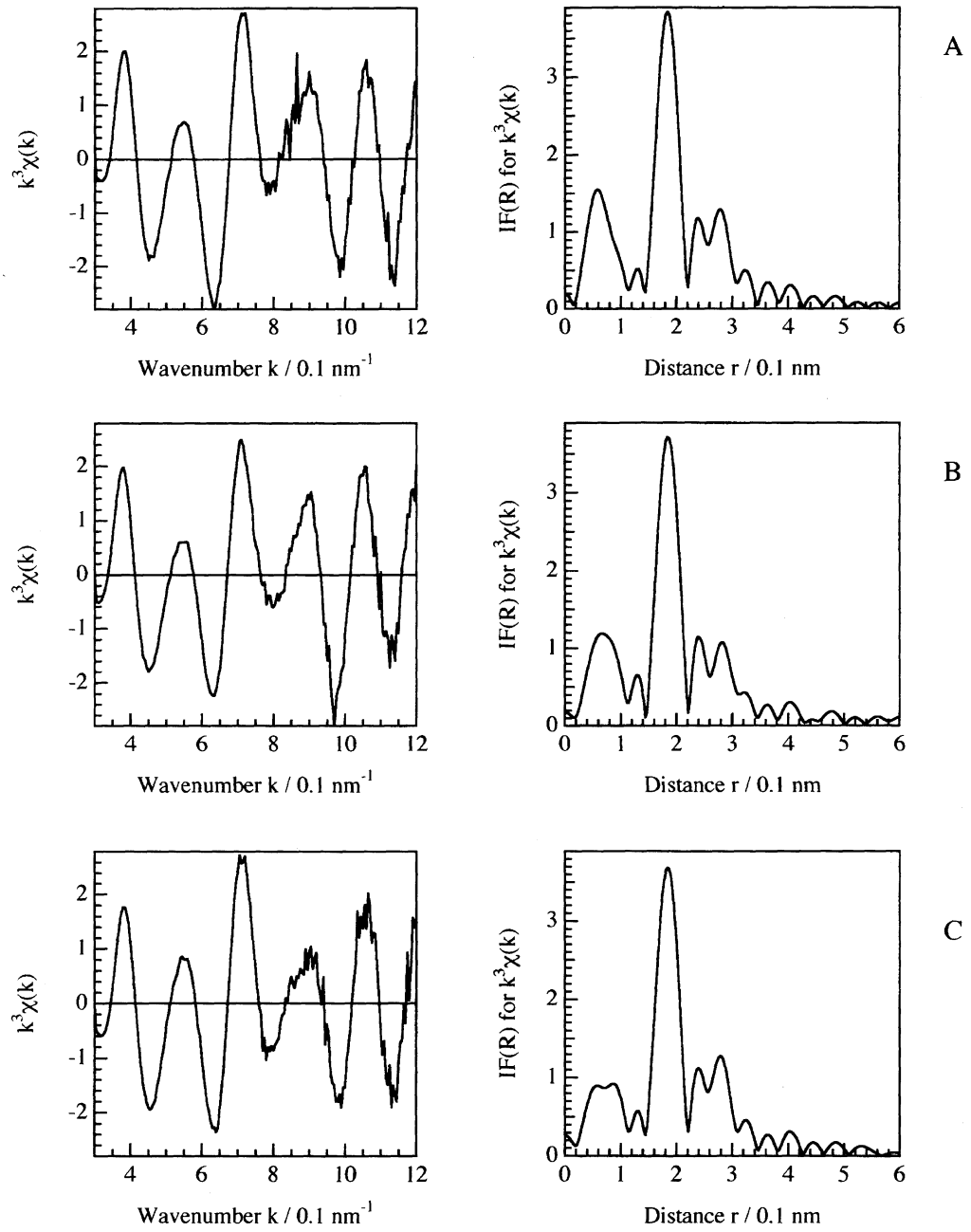

Fig. 6. Au L_3-edge EXAFS oscillations and associated Fourier transforms for **1**/SiO_2. (A) **1**/SiO_2; (B) **1**/SiO_2 under 300 Torr of CO; (C) **1**/SiO_2 after evacuation at 353 K.

Table 3. Curve-Fitting Results for the Au L_3-edge EXAFS Data of **1**/SiO_2

Sample	Au–P		Au–Pt		Au–Au	
	N	*r*/nm	*N*	*r*/nm	*N*	*r*/nm
1	1[a)]	0.229[a)]	1[a)]	0.268[a)]	2.67[a)]	0.285[a)]
3	1[a)]	0.229[a)]	1[a)]	0.269[a)]	3[a)]	0.289[a)]
1/SiO_2	1.0±0.1	0.228±0.001	1.1±0.1	0.268±0.001	2.6±0.3	0.285±0.001
1/SiO_2 after adsorption of CO	1.0±0.1	0.228±0.004	1.1±0.1	0.269±0.001	3.0±0.3	0.290±0.001
1/SiO_2 after desorption of CO	1.0±0.1	0.228±0.001	1.1±0.1	0.268±0.001	2.7±0.3	0.285±0.001

The Δr range for the inverse Fourier transformation was 0.12—0.35 nm for both Pt and Au EXAFS. The curve fitting range was 30—120 nm^{-1} for Au EXAFS. a) The averaged values derived from crystallographic data.[30]

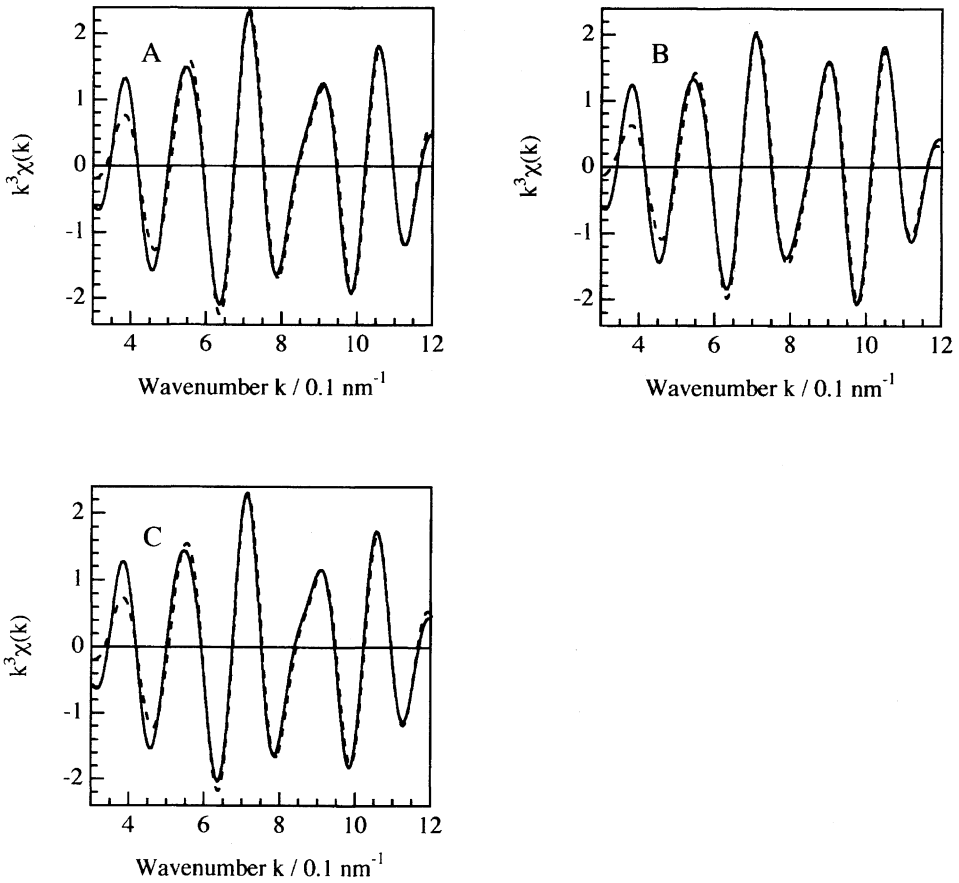

Fig. 7. The curve-fitting analysis for the Au L_3-edge EXAFS data of **1**/SiO_2 based on two-shells model (Au–P and Au–Au(Pt)): —, observed, ····, calculated. (A) **1**/SiO_2; (B) **1**/SiO_2 after adsorption of CO; (C) **1**/SiO_2 after desorption of the adsorbed CO at 353 K.

transforms for the EXAFS data at Pt L_3-edge and Au L_3-edge for **1**/SiO_2 before exposure to H_2, under 0.3 MPa of H_2 and after evacuation, respectively. It was found that the EXASF spectra were quite similar to each other. There was little difference in the cluster structures among the three samples.

Discussion

CO Adsorption on 1/SiO_2. From comparison with the crystal data and ν_{CO} peak of the cluster $[(AuPPh_3)_6Pt(CO)(PPh_3)]^{2+}$ synthesized by reaction of **1** with CO in solution, the peak at 1972 cm^{-1} observed with the CO-adsorbed **1**/SiO_2 is assigned to linear CO adsorbed on Pt. When CO was exposed to the **1**/SiO_2 pretreated at 473 K, the ν_{CO} peak became slightly weaker in intensity and higher in wavenumber in Fig. 1B and the TPD-desorption amount of CO became smaller in Fig. 2A. These results support the indication of the previous EXFAS results that there is a small deformation in the cluster framework by heating the intact **1**/SiO_2 at 473 K in vacuum, where the bond numbers of Au–Au(Pt) and Pt–Au decreased to about 75 and 68% of the original ones.[13,15]

Structure Transformation of 1/SiO_2 by CO Adsorption and Desorption. We have observed a reversible structure transformation of **1**/SiO_2 by the adsorption and desorption of CO without any fragmentation of the Au_6Pt framework. There are two features in this transformation found by EXAFS: (1) The Au–Au coordination number increases with the CO adsorption; (2) The peak of Pt–(Au)–P in the Fourier transform of Pt L_3-edge increases, though no increase in the coordination number of P around Au is observed. Thus the change occurs only on the Au atoms surrounding Pt.

A CO-adduct cluster $[(AuPPh_3)_6Pt(CO)(PPh_3)](PF_6)_2$ (**3**) can be easily derived by reaction of **1** with CO in CH_2Cl_2 solution and thereafter by metathesis of NO_3^- salt from a methanol solution of NH_4PF_6.[30] The compound **3** has a longer Pt–P bond distance on average than the cluster **1**, which is compatible with the change found in the cluster **1** on SiO_2 after CO adsorption, as shown in Table 2.

The increase in the Pt–(Au)–P Fourier transform peak intensity can be explained by the bond angle of Pt–Au–P to be 180°, which causes a strong focusing effect in the multi scattering of photoelectrons. The average angles of Pt–Au–P in clusters **1** and **3** are 162.5° and 164.8°, respectively, based on the crystallographic data. We have calculated the Pt–(Au)–P EXAFS oscillation using the FEFF program on the assumption that the cluster structures on SiO_2 before and after CO adsorption are the same as the ones in compounds **1** and **3** given in the literature, respectively.[30] The results are depicted in Fig. 10. Because of the ambiguity in Debye–Waller factors, the relative height of the simulated Fourier transforms has some meaning. The height around 0.45 nm in **1** is 1.1 and it increases to 2.0 in **3**. Therefore, the increase in the

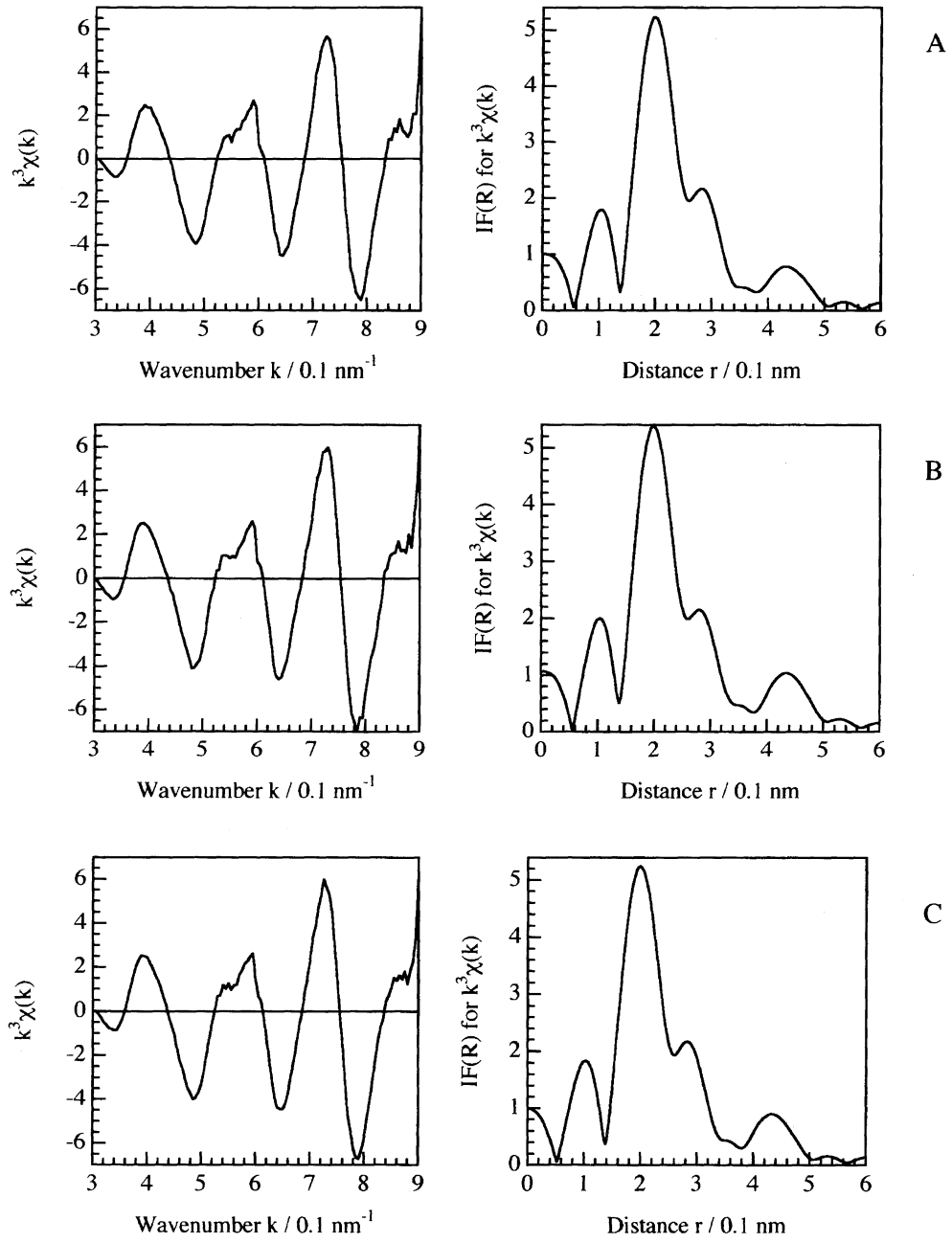

Fig. 8. Pt L_3-edge EXAFS oscillations and associated Fourier transforms for **1**/SiO_2. (A) **1**/SiO_2; (B) **1**/SiO_2 under 0.3 MPa of H_2; (C) **1**/SiO_2 after desorption of H_2.

peak of 0.45 nm in the Pt L_3-edge EXAFS Fourier transform (Fig. 4) can be explained by the transformation of the surface structure from **1** to **3** by the CO adsorption. Note that the difference in average Pt–Au–P angle between **1** and **3** is 2.3°, though the peak height for **3** is almost twice that for **1**. According to the FEFF calculation of the peak height of Pt–(Au)–P in the Fourier transform for several angles, the peak height sensitively varied with the angles at larger than 160°.

From the EXAFS results, we propose that the structure transformation occurs during CO adsorption, as shown in Fig. 11. It is to be noted that the adsorption of CO from Pt atom has never been observed with the cluster **3** in a solution system unless the framework structure is destroyed. Supporting the cluster **1** on SiO_2 has made it possible to undergo a reversible structural change without collapse of the cluster framework like $Ru_6C(CO)_{16}$/MgO.[31] Such a reversible structural change may provide a molecular actuator for molecular mechanics and molecular devices.

Adsorption of H_2 and Mechanism Consideration of H_2–D_2 Equilibration on 1/SiO_2. It has been reported that the cluster **1** showed a catalytic activity with TOFs of 0.6 s^{-1} in solution and 2.0 s^{-1} in gas-solid condition for H_2–D_2 equilibration at room temperature. It was also found that the TOF increased to 29.8 s^{-1} by supporting **1** on SiO_2, mainly due to high dispersion of the active clusters where the reaction occurs on the Pt atom promoted by Au–Pt bonds.[12–15] When H_2 was exposed to the intact **1**/SiO_2, however, only

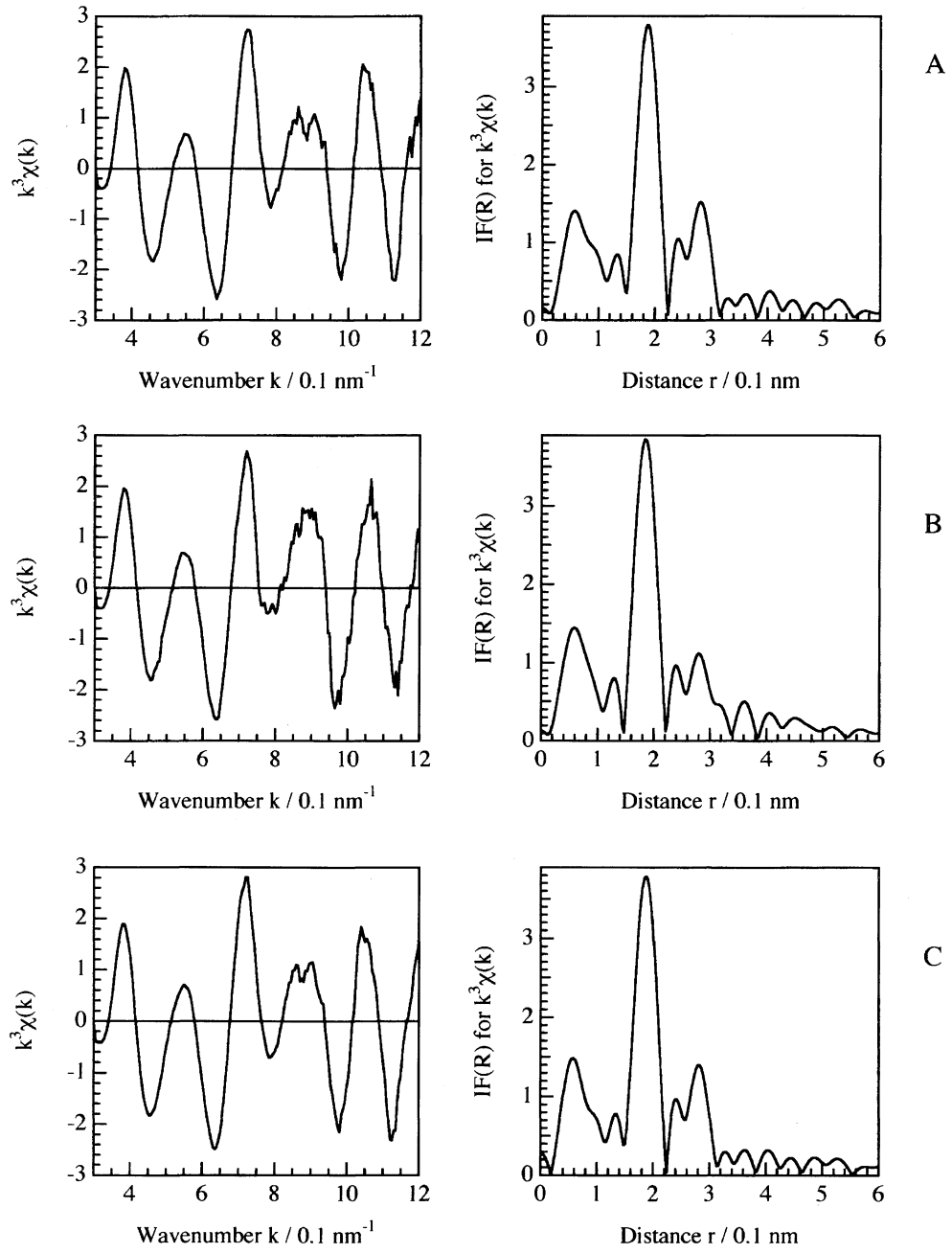

Fig. 9. Au L_3-edge EXAFS oscillations and associated Fourier transforms for **1**/SiO_2. (A) **1**/SiO_2; (B) **1**/SiO_2 under 0.3 MPa of H_2; (C) **1**/SiO_2 after desorption of H_2.

very weak adsorption of H_2 on **1**/SiO_2 occurred and almost no contribution of H_2 adsorption to the EXAFS observation was observed. It is not due to the weak scattering of hydrogen. Kubota et al. reported that a shape change 8 eV above the edge occurred when hydrogen was adsorbed on Pt.[32] They attributed the shape change to a multiple scattering effect caused by H–Pt bonds.[33] Koningsberger ascribed the change to an EXAFS structure based on their FEFF calculations.[34] Thus if hydrogen was chemisorbed on Pt, one should find a change near the edge region. However, we could not find any change in the edge region of **1**/SiO_2 and no dissociative chemisorption occurred, but very weak adsorption of H_2 on **1**/SiO_2 did occurr.

The structure transformation of **1**/SiO_2 by CO adsorption and desorption encouraged us to examine the possibility that H_2 adsorption or H_2–D_2 equilibration on **1**/SiO_2 may result in core movements of the cluster framework through the angle of Pt–Au–P and the bond length of Au–Pt(Au). Recently, a B3LYP study was performed on the phosphine-ligated gold-platinum model clusters such as $[(AuPH_3)_6Pt(PH_3)]^{2+}$ and $[(AuPH_3)_6Pt(H_2)(PH_3)]^{2+}$.[35] The theoretical calculation revealed that there were two stable H_2 adducts (dihydrogen complexes), which might be possible intermediates for the H_2–D_2 equilibration. The potential profile along the reaction path was very flat. Pt was characterized as being the active site, but Au atoms also played an important role in H_2 acti-

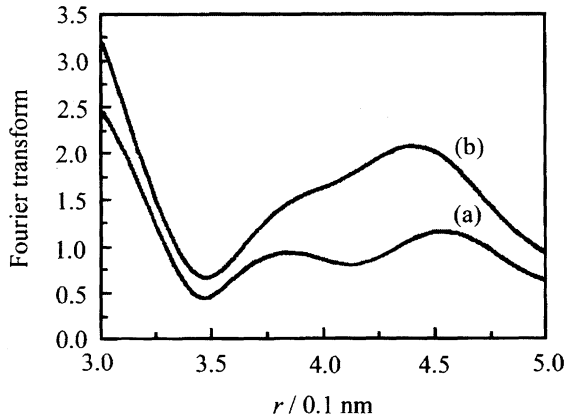

Fig. 10. Fourier transforms of the FEFF simulation based on the models **1** (a) and **3** (b). The Fourier transformation was carried out over k = 30—90 nm^{-1}.

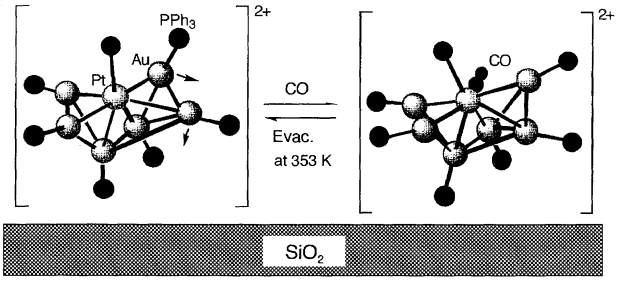

Fig. 11. Structural transformation of **1**/SiO_2 by CO adsorption and desorption.

vation. The H_2 activation may include the electron transfer from the metal core to the σ^* anti-bonding orbital of H_2 and movements of the metal core.[35] These findings support the experimental fact that the reaction between **1**/SiO_2 and H_2 is a rapid reversible reaction.

Conclusion

The SiO_2-supported cluster $[(AuPPh_3)_6Pt(PPh_3)](NO_3)_2$ (**1**) reacted with CO on the Pt atom to give a CO-adduct **1**/SiO_2, which showed ν_{CO} at 1972 cm^{-1}. One CO molecule adsorbed on a Pt atom in **1**/SiO_2 when the CO pressure was higher than 250 Torr. The cluster framework of **1** on SiO_2 was deformed by the expansion in the bond angle of ∠Au–Pt–P when CO adsorbed on the Pt atom of **1**/SiO_2. The deformed structure was reconverted to the original structure without fragmentation by evacuation of CO at 353 K, unlike the case of the cluster in solution. The SiO_2 surface prevented the bimetal cluster structure from fragmenting during the adsorption–desorption process. The H_2 adsorption on **1**/SiO_2 was weak and reversible at 298 K. The contribution of H_2 to the EXAFS of **1**/SiO_2 was negligible.

This work has been supported by Core Research for Evolutional Science and Technology (CREST) of the Japan Science and Technology Corporation (JST). The EXAFS measurements have been performed with approval of the Photon Factory Advisory Committee (Proposal No. 95G200).

References

1 For examples of supported Au catalysts: a) N. W. Cant and W. K. Hall, *J. Phys. Chem.*, **75**, 2914 (1995). b) S. Galvagno and G. Parravano, *J. Catal.*, **55**, 178 (1978). c) J. Schwank, *Gold Bull.*, **16**, 103 (1983). d) M. Haruta, S. Tsubota, N. Yamada, T. Kobayashi, and S. Iijima, *J. Catal.*, **115**, 301 (1989). e) S. D. Gardner and G. B. Hoflund, *Langmuir*, **7**, 2135 (1991). f) S. D. Gardner, G. B. Hoflund, and M. R. Davidson, *Langmuir*, **7**, 2140 (1991). g) M. Haruta, S. Tsubota, T. Kobayashi, H. Kageyama, M. J. Genet, and B. Delmon, *J. Catal.*, **144**, 174 (1993). h) S. Tsubota, A. Ueda, H. Sakurai, T. Kabayashi, and M. Haruta, *ACS Symp. Ser.*, **552**, 420 (1993). i) G. B. Hoflund, S. D. Gardner, D. R. Schryer, B. T. Upchurch, and E. J. Kielin, *Appl. Catal.*, **6**, 117 (1995). j) G. Srinivas, J. Wright, C.-S. Bai, and R. Cook, *Stud. Surf. Sci. Catal.*, **101**, 427 (1996). k) Y. Yuan, K. Asakura, H. Wan, K. Tsai, and Y. Iwasawa, *Catal. Lett.*, **42**, 15 (1996). l) Y. Yuan, K. Asakura, H. Wan, K. Tsai, and Y. Iwasawa, *Chem. Lett.*, **29**, 755 (1996). m) Y. Yuan, A. P. Kozlova, K. Asakura, H. Wan, K. Tsai, and Y. Iwasawa, *J. Catal.*, **170**, 191 (1997). n) Y. Yuan, K. Asakura, A. P. Kozlova, H. Wan, K. Tsai, and Y. Iwasawa, *Catal. Today*, **44**, 333 (1998).

2 For Examples of Pt-transition metal catalysts: a) Y. L. Lam and M. Boudart, *J. Catal.*, **50**, 530 (1977). b) Y. L. Lam, J. Criado, and M. Boudart, *Nouv. J. Chim.*, **1**, 461 (1977). c) G. A. Somorjai, *Catal. Lett.*, **15**, 25 (1992). d) W. D. Provine, P. L. Mills, and J. J. Lerou, *Stud. Surf. Sci. Catal.*, **101**, 191 (1996).

3 For examples of Pt–Au catalysts: a) J. R. H. van Schaik, R. P. Dessing, and V. Ponec, *J. Catal.*, **38**, 273 (1975). b) J. K. A. Clarke, L. Manninger, and T. Baird, *J. Catal.*, **54**, 230 (1978). c) J. K. A. Clarke, L. Manninger, and T. Baird, *J. Catal.*, **9**, 85 (1984). d) J. H. Sinfelt, "Bimetallic Catalysts," Wiley, New York (1985). e) R. C. Yates and G. A. Somorjai, *J. Catal.*, **103**, 208 (1987). f) K. Balakrishnan, A. Sachdev, and J. Sachwank, *J. Catal.*, **121**, 441 (1990). g) P. A. Sermon, J. M. Thomas, K. Keryou, and G. R. Millward, *Angew. Chem., Int. Ed. Engl.*, **26**, 918 (1987). h) A. Sachdev and J. Schwank, *J. Catal.*, **120**, 353 (1989). i) K. Balakrishnan and J. Sachwank, *J. Catal.*, **132**, 451 (1991). j) D. Rouabah and J. Fraissard, *J. Catal.*, **144**, 30 (1993). k) J. Sachtler, K. Balakrishnan, and A. Sachdev, in "New Frontiers in Catalysis," ed by L. Guczi, F. Solymosi, and P. Tetenyi, Elservier, Amsterdam (1993), p. 905.

4 J. W. A Sachtler and G. A. Somorjai, *J. Catal.*, **81**, 77 (1983).

5 J. Sachlter, J. Biberian, and G. Somorjai, *Surf. Sci.*, **110**, 43 (1981).

6 A. Sachdev and J. Schwank, *J. Catal.*, **120**, 353 (1989).

7 J. R. H. van Shaik, R. P. Dessing, and V. Ponec, *J. Catal.*, **38**, 273 (1975).

8 H. C. de Jongste, F. J. Kuijers, and V. Ponec, in "Proc. Int. Symp. Heterogeneous Catalysis," ed by B. Delmon, P. A. Jacobs, and G. Poncelet, Brussels (1975), Elsevier, Amsterdam (1976), p. 207.

9 R. P. Dessing and V. Ponec, *React. Kinet. Catal. Lett.*, **5**, 251 (1976).

10 A. F. Kane and J. K. A. Clarke, *J. Chem. Soc., Faraday Trans. 1*, **76**, 1640 (1980).

11 J. K. A. Clarke, I. Manninger, and T. Baird, *J. Catal.*, **54**, 230 (1978).

12 I. Gubkina, L. Rubinstein, and L. Pignolet, *Abstr. of ACS Meeting*, **208**, 405 (1994).

13 Y. Yuan, K. Asakura, H. Wan, K. Tsai, and Y. Iwasawa, *Chem. Lett.*, **1996**, 129.

14 I. V. G. Graf, J. W. Bacon, M. B. Consugar, M. E. Curley, L. N. Ito, and L. H. Pignolet, *Inorg. Chem.*, **35**, 689 (1996).

15 Y. Yuan, K. Asakura, H. Wan, K. Tsai, and Y. Iwasawa, *J. Mol. Catal. A: Chem.*, **122**, 147 (1997).

16 M. A. Aubart, B. D. Chandler, R. A. T. Gould, D. A. Krogstad, M. F. J. Schoondergang, and L. H. Pignolet, *Inorg. Chem.*, **33**, 3724 (1994).

17 D. C. Roe, *J. Magn. Res.*, **63**, 388 (1985).

18 T. G. M. M. Kappen, J. J. Bour, P. P. J. Schlebos, A. M. Reolofsen, J. G. M. van der Linden, J. J. Steggerda, M. A. Aubart, D. A. Krogstad, M. F. J. Schoonderhang, and L. H. Pignolet, *Inorg. Chem.*, **32**, 1074 (1993).

19 J. J. Bour, P. P. J. Schlebos, R. P. F. Kanters, M. F. J. Schoondergang, H. Addens, A. Overweg, and J. J. Steggerda, *Inorg. Chim. Acta*, **181**, 195 (1991).

20 M. A. Aubart, J. F. D. Koch, and L. H. Pignolet, *Inorg. Chem.*, **33**, 3852 (1994).

21 Y. Iwasawa, *Stud. Surf. Sci. Catal.* (Proc. 11th Int. Congr. Catal., Baltimore), Vol. 101, Elsevier (1996), p. 21.

22 Y. Iwasawa, "Tailored Metal Catalysts," Reidel, Holland (1986).

23 Y. Iwasawa, *Adv. Catal.*, **35**, 187 (1987).

24 Y. Iwasawa, *Catal. Today*, **18**, 21 (1993).

25 Y. Iwasawa, "X-Ray Adsorption Fine Structure for Catalysts and Surfaces," World Scientific, Singapore (1996).

26 Y. Iwasawa, *Res. Chem. Intermed.*, **15**, 183 (1991).

27 K. Asakura, Y. Yuan, and Y. Iwasawa, *J. Phys. IV, Fr.*, **7**, C2-863 (1997).

28 K. Asakura, in "X-Ray Adsorption Fine Structure for Catalysts and Surfaces," ed by Y. Iwasawa, World Scientific, Singapore (1996).

29 J. J. Rehr, de Leon, J. Mustre, S. I. Zabinsky, and R. C. Albers, *J. Am. Chem. Soc.*, **113**, 5235 (1991).

30 L. N. Ito, J. D. Sweet, A. M. Mueting, L. H. Pignolet, M. F. J. Schoodergang, and J. J. Steggerda, *Inorg. Chem.*, **28**, 3696 (1989).

31 Y. Izumi, T. Chihara, H. Yamazaki, and Y. Iwasawa, *J. Chem. Soc., Dalton Trans.*, **1993**, 3667.

32 T. Kubota, K. Asakura, N. Ichikuni, and Y. Iwasawa, *Chem. Phys. Lett.*, **256**, 445 (1996).

33 K. Ohtani, T. Fujikawa, T. Kubota, K. Asakura, and Y. Iwasawa, *Jpn. J. Appl. Phys.*, **36**, 6504 (1997).

34 D.C. Konigsberger, *Proc. XAFS X*, in press.

35 X. Xu, Y. Yuan, K. Asakura, Y. Iwasawa, H. Wan, and K. Tsai, *Chem. Phys. Lett.*, **286**, 163 (1998).